J Mater Sci: Mater Med (2008) 19:1999–2008
DOI 10.1007/s10856-007-3277-1

Equilibrium and non-equilibrium charge-dependent quantification of endothelial cell hydrogel scaffolds

Kari B. Haxhinasto · Anthony E. English · Alan B. Moy

Received: 28 June 2007 / Accepted: 10 September 2007 / Published online: 18 October 2007

Abstract Using equilibrium swelling and non-equilibrium membrane potential measurements, this study assesses the charge density in two representative series of polyelectrolyte hydrogels and examines the morphological and proliferative responses of endothelial cells as a function of the prepared charge offset. The neutral monomers 2-hydroxyethylmethacrylate (HEMA) and poly(ethylene glycol) dimethacrylate (n = 1,000) (PEGDMA) were copolymerized with either the acidic monomer 2-sulfoethyl methacrylate (SEMA) or the basic monomer methacryloxy ethyltrimethylammonium chloride (MAETAC) to make membranes with pregelation charge offset concentrations varying from 0 to ±200 mM. A thermodynamic analysis of swelling and membrane potential measurements quantified the hydrogel charge density state following equilibration at different ion strengths. Porcine pulmonary artery endothelial cells were seeded on samples of each HEMA and PEGDMA copolymer and the amount of cell coverage was measured over a 4-day period. Cellular attachment and proliferation increased with increasing proportions of charged monomers and showed a threshold pattern of attachment and growth on the positively charged HEMA–MAETAC copolymer hydrogels with increasing proportions of initially prepared charge. The series of PEGDMA copolymer hydrogels remained relatively resistant to cellular attachment and proliferation over the range of prepared charges considered in this study.

K. B. Haxhinasto · A. E. English (✉)
Department of Mechanical, Aerospace and Biomedical Engineering, The University of Tennessee, 308 Perkins Hall, Knoxville, TN 37996, USA
e-mail: tenglish@utk.edu

A. B. Moy
Cellular Engineering Technologies, Coralville, IA 52241, USA

1 Introduction

Natural and synthetic hydrogels with charged monomeric groups have found many applications in vascular tissue engineering. The adhesion of endothelial cells to each other and to their underlying matrix plays a critical role in the optimal development of tissue engineered vascular constructs and in the etiology of many cardiovascular, respiratory, and renal complications. Endothelial cell matrix interactions, in particular, play a role in cell proliferation, spreading, and morphology, as well as in various pathological processes. Methods for promoting cellular attachment to biomaterials are, therefore, central to many tissue engineering applications as well as to a basic understanding of disease processes.

The incorporation of charged functional groups into an otherwise neutral and inert polymer background has been exploited to promote endothelial cell adhesion and proliferation [1–3]. Charged functional groups in synthetic and natural matrices not only contribute to the necessary non-specific interactions required for cell attachment, but they also contribute to specific binding interactions. The effective surface charge promotes the absorption of proteins that can present specific binding sites to cell membrane receptors. Some charged monomeric groups are actually used for further synthesis steps to attach specific cellular adhesion molecules.

Attempting to optimize cellular attachment and proliferation by altering the composition of the hydrogel matrix is a complex task. Adding charged monomers to a neutral polymer network, for example, can produce swelling transitions that significantly alter the hydrogel state [4–9]. The effective charge, therefore, can be very different from the starting monomer concentrations used to prepare the hydrogel. Entanglement, solvent effects, cross-linking

density, and many other factors can influence the final equilibrium swelling and charge state. Quantitative hydrogel thermodynamic models that include these effects have a great deal of potential when integrated with more traditional models of cell–matrix attachment [10–13]. A careful balance of experimental and theoretical methods, however, is necessary in order to successfully couple complex matrix thermodynamic state transitions with cellular binding.

This study applies a combination of equilibrium swelling and non-equilibrium membrane potential measurements to define both the matrix charge density following equilibration at physiologic ion strengths and its effect on cellular proliferation and morphology. Specifically, this study investigates the cellular proliferation and morphology of porcine pulmonary artery endothelial cells (PPAECs) on copolymer hydrogels with varying positive and negative charge offsets. Hydrogels composed of HEMA or PEG-DMA (n = 1,000), copolymerized with the strongly charged acidic and basic moieties, 2-sulfoethyl methacrylate (SEMA) and methacryloxyethyl trimethyl ammonium chloride (MAETAC), respectively, served as cellular scaffolds for the investigation of charge-dependent proliferation and morphology.

2 Theoretical model

2.1 Equilibrium swelling

The total system Helmholtz free energy can be written as a sum of a hydrogel and a bath free energy component, i.e.,

$$\Delta F^{\mathrm{T}} = \Delta F + \Delta F^{B}, \tag{1}$$

where ΔF and ΔF^{B} represent the hydrogel and bath components, respectively. The hydrogel Helmholtz free energy can be represented as a sum of the three components

$$\Delta F = \Delta F_{\mathrm{M}} + \Delta F_{\mathrm{el}} + \Delta F_{0}, \tag{2}$$

where ΔF_{M}, ΔF_{el}, and ΔF_{M} represent the mixing, elastic, and mobile particle free energy contributions to the hydrogel Helmholtz free energy, respectively. As described in previous studies [6–8], these three terms can be written as

$$\Delta F_{\mathrm{M}} = k_{\mathrm{B}}T\frac{V}{v}(1-nv)[\ln(1-nv)+\chi nv], \tag{3}$$

$$\Delta F_{\mathrm{el}} = \frac{3k_{\mathrm{B}}T}{2}\frac{Vn}{N_x}\left[\left(\frac{n_0}{n}\right)^{2/3} - 1 - \frac{1}{3}\ln\left(\frac{n_0}{n}\right)\right], \tag{4}$$

and

$$\Delta F_{0} = k_{\mathrm{B}}T\sum_{i=1}^{\sigma} N_i\left\{\ln\left(\frac{N_i}{V}\right) - 1\right\} + \sum_{i=1}^{\sigma} z_i e N_i \varphi_0, \tag{5}$$

where v is the lattice site volume, n the monomer concentration, χ the Flory interaction parameter, k_{B} is the Boltzmann constant, and T the absolute temperature. The term N_x represents the average number of monomers between cross-links, Vn/N_x is the effective number of chains in the network, and n_0/n is the swelling ratio. Also, N_i represents the total number of the ith mobile particle within the hydrogel, z_i is the ith ion valence, e represents the unit charge, and φ_0 is the uniform component of the electrostatic potential energy created by the hydrogel interfacial boundary. The bath Helmholtz free energy is simply equal to the translational free energy of the ions in a uniform potential, i.e.,

$$\Delta F^{\mathrm{B}} = k_{\mathrm{B}}T\sum_{i=1}^{\sigma} N_i^{\mathrm{B}}\left\{\ln\left(\frac{N_i^{\mathrm{B}}}{V^{\mathrm{B}}}\right) - 1\right\} + \sum_{i=1}^{\sigma} z_i e N_i^{\mathrm{B}} \varphi_0^{\mathrm{B}}. \tag{6}$$

The equilibrium states follow from the extremum of the internal degrees of freedom [14]. Swelling equilibrium is given by

$$0 = -\frac{1}{v}\left[\ln(1-nv) + nv + \chi(nv)^2\right] + \frac{n_0}{N_x v_{\mathrm{site}}}\left[\frac{1}{2}\left(\frac{n}{n_0}\right) - \left(\frac{n}{n_0}\right)^{1/3}\right] + \sum_{i=0}^{\sigma} c_i - \sum_{i=0}^{\sigma} c_i^{\mathrm{B}}, \tag{7}$$

where $v = N_{\mathrm{A}}\, v_{\mathrm{site}}$ represents the molar volume of the lattice sites. The balance of ion chemical potentials is equivalent to the Donnan relations,

$$\left(\frac{C_i}{C_i^{\mathrm{B}}}\right)^{\frac{1}{z_i}} = \left(\frac{C_j}{C_j^{\mathrm{B}}}\right)^{\frac{1}{z_j}} = 0. \tag{8}$$

The effects of ion dissociation can be ignored in this case since we are dealing with strongly basic and acidic monomers.

2.2 Non-equilibrium steady-state membrane potentials

As illustrated in Fig. 1, a hydrogel membrane with charge density $\overline{\rho}$ separating two reservoirs with salt concentrations C^1 and C^2, respectively, produces a charge dependent potential, $\Delta\Phi_{\mathrm{M}}$. Based on the Teroell-Mayer-Severs (TMS) model, the total potential produced by a membrane, of thickness d, is a sum of two membrane interfacial potentials and a diffusion potential such that

$$\Delta\Phi_{\mathrm{M}} = \Delta\Phi(0) + \Delta\Phi_{\mathrm{Diff}} + \Delta\Phi(d), \tag{9}$$

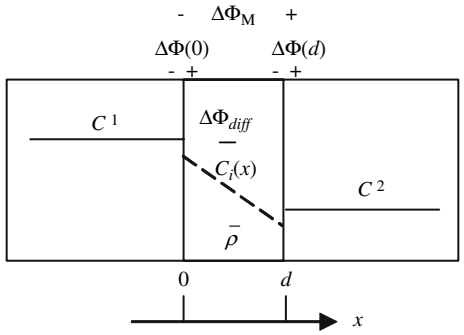

Fig. 1 Steady-state membrane potential components based on the TMS model. A salt concentration gradient is applied across a membrane of thickness, d, by maintaining a concentration C^1 in chamber 1 and a concentration C^2 in chamber 2. The total membrane potential, Φ_M, consists of interfacial potentials, $\Phi(0)$ and $\Phi(d)$, at each membrane boundary and a diffusion potential term Φ_{diff}. The fixed membrane charge density, $\overline{\rho}$, produces the interfacial potentials at each boundary and a spatially dependent concentration, $\overline{C}_i(x)$, for the ith ion. The concentration, $\overline{C}_i(x)$, will also depend on the ith ion valence

where $\Delta\Phi(0)$ is the interfacial potential drop at $x = 0$, $\Delta\Phi(d)$ is the interfacial potential drop at $x = d$, and $\Delta\Phi_{Diff}$ is the diffusion potential.

At each membrane–solution interface, the sum of the Nernst potentials for ions of the same charge can be set equal to a charge density relation, using the conditions of electroneutrality, thus forming two equations. The equation for the left interface is

$$r^1 = \sum \left(\frac{\overline{C}_+^1}{C_+^1}\right)^{\frac{1}{z_+}} = \sum \left(\frac{\overline{C}_-^1}{C_-^1}\right)^{\frac{1}{z_-}} = \sqrt{1+\left(\frac{\overline{\rho}/F}{2C^1}\right)^2} - \frac{\overline{\rho}/F}{2C^1}, \tag{10}$$

where the over-bars denote the membrane phase and r represents the Donnan ratio. The equation for the right interface is

$$r^2 = \sum \left(\frac{\overline{C}_+^2}{C_+^2}\right)^{\frac{1}{z_+}} = \sum \left(\frac{\overline{C}_-^2}{C_-^2}\right)^{\frac{1}{z_-}} = \sqrt{1+\left(\frac{\overline{\rho}/F}{2C^2}\right)^2} - \frac{\overline{\rho}/F}{2C^2}, \tag{11}$$

where it is assumed that the concentration taken just inside and just outside the membrane interface are several Debye lengths away from the interface itself. Knowing these relationships, the potential drop across the membrane caused by the Donnan effect is equal to,

$$\Delta V_D = \Delta\Phi(0) + \Delta\Phi(d) = -\frac{RT}{F}\ln\frac{r^2}{r^1}. \tag{12}$$

The potential drop caused by the diffusion potential can be estimated using the Henderson equation. The Henderson equation models a continuous series of mixtures brought together in the diffusion zone. Here, the zone is the membrane and at any point within it, species i has a concentration, $\overline{C}_i$. Then, $\overline{C}_i^1$ and $\overline{C}_i^2$ represent the concentrations of species i just inside the left and right membrane–solution interfaces, respectively. Then,

$$\overline{C}_i = \overline{C}_i^1(1-x) + \overline{C}_i^2 x, \tag{13}$$

where x is the fraction of solution 2, and $(1–x)$ is the fraction of solution 1 at the given point. The activities for each ion are then substituted by their respective concentrations, and their mobilities are assumed to be independent of concentration. For a binary electrolyte, this reduces to

$$\Delta\Phi_{diff} = -\frac{RT}{zF}\left(\frac{D_+ - D_-}{D_+ + D_-}\right)\ln\left(\frac{C^2}{C^1}\right), \tag{14}$$

where D_+ is the cation diffusion coefficient, D_- is the anion diffusion coefficient, and z is the absolute value of the ion valence. The total measured potential difference, therefore, is the sum of V_D and V_d such that

$$\Delta\Phi_M = \Delta\Phi_{diff} + \left(\frac{RT}{F}\right)\ln\frac{r^2}{r^1}. \tag{15}$$

3 Materials and methods

3.1 Hydrogel preparation and swelling measurements

Copolymer hydrogels were synthesized using the monomers 2-sulfoethyl methacrylate (SEMA) or 2-methacryloxyethyltrimethylammonium chloride (MAETAC) mixed in varying proportions with the neutral monomers, 2-hydroxyethyl methacrylate (HEMA) and poly(ethylene glycol) (1000) dimethacrylate (PEGDMA). Specifically, a 2 M HEMA or PEGDMA solution was mixed with one of the 2 M charged monomer stock solutions to yield a total volume of 10 mL in proportions that produced charge offsets ranging from –200 mM to +200 mM in 40 mM increments. The charged monomers SEMA and MAETAC were very strong acids and bases, respectively. Hence, the charged copolymers reduced the complications produced by the acid–base dissociation.

The copolymer hydrogels were cut into 78.5 mm^2 circular discs and equilibrated in phosphate buffer saline (PBS). The hydrogels were then autoclaved in media bottles in preparation for testing. Experimental procedures were carried out under a culture hood with sterile apparatus to avoid infection. Four gels of each charge concentration, including HEMA and PEGDMA at charge concentrations of 0–200 mM in increments of 40 mM, were taken from

their respective media bottles with sterile tweezers. Each gel was immediately placed in one well of a 12-well tissue culture dish along with 2 mL of M199 with 10% fetal bovine serum (FBS) and supplements. Six wells were left empty as controls. One hydrogel of each charge concentration, including HEMA and PEGDMA, was taken from its respective media bottle with sterile tweezers and placed in one well of a 12-well tissue culture dish along with 2 mL of M199 with supplements, but without FBS. All gels were then left to equilibrate for 16 h. To obtain swelling estimates, hydrogel disc diameters were measured immediately after casting and following equilibration. The swelling was recorded as the new equilibrium diameter divided by the original hydrogel diameter.

3.2 Endothelial cell isolation and culturing

Endothelial cells were isolated from porcine pulmonary arteries obtained from a local abattoir. The endothelial cells were cultivated in an incubator at 37 °C and 5% CO_2. The cell culture media consisted of M199 (GibcoBRL) and 10% fetal bovine serum (Hyclone) supplemented with vitamins (Sigma), glutamine (GibcoBRL), penicillin and streptomycin (GibcoBRL), and amino acids (Sigma). The isolated cells had a cobblestone morphology and LDL uptake characteristic of endothelial cells. Passages between 4 and 8 were used for this study.

Endothelial cells were trypsinized using 0.05% trypsin–EDTA and counted using a hemocytometer. The cells were then spun down in a sterile 15 mL centrifuge tube for 5 min at 800 rpm. The trypsin was then drawn off and the cell pellet was resuspended via rapid pipetting with 10 mL M199. From these cell solutions, 1 mL was taken and used to inoculate each hydrogel disc with approximately 10^5 cells. Three samples at each different composition were used. Two groups of controls, one for the HEMA copolymers and one for the PEGDMA copolymers, were included by inoculating the bottom of six wells without gels. This ensured that cells attached, proliferated, and formed a confluent layer across the bottom of the tissue culture wells. The remaining sets of HEMA and PEGDMA copolymers, including the gels equilibrated in non-serum media, were not inoculated; instead, they were used as control groups in the membrane potential measurements. The medium in each well was changed every 2 days and all membrane potential measurements were carried out 5 days after inoculation.

3.3 Imaging

The quantification of endothelial cell proliferation on the HEMA and PEGDMA copolymers was obtained by analyzing pictures taken using a microscope equipped with a charge-coupled device camera. Three pictures were taken of representative fields of three different hydrogels of each charge at 4, 24, 48, 72, and 96 h post-inoculation. The area of cell coverage per picture was measured using software tools in Scion Image by outlining either the attached cells or the bare surfaces and adding these values. These data were then normalized to the total area represented in one picture and presented in graphical form, with 1.0 representing 100% complete cell coverage, or cell confluence, and 0% representing no cell coverage, or cell death.

3.4 Hydrogel membrane potential measurements

Membrane potential measurements were made with both sets of HEMA and PEGDMA copolymers using a high-input impedance electrometer (World Precision International EVC4000). Chamber 1 was filled with 154 mM NaCl, and chamber 2 was filled with logarithmically spaced concentrations of NaCl solutions. The apical surface faced chamber 1 during all membrane potential experiments. The hydrogels, which had been inoculated with cells, were measured first to investigate the possible variability in charge as a result of the cell monolayer, cellular matrix deposits, or adhered proteins from the media. Endothelial cell seeded membranes were checked before and after membrane potential measurements to ensure that endothelial cells were attached. The non-inoculated hydrogels equilibrated in media with and without serum were used as controls. Membrane potential measurements were performed on these hydrogels to provide a comparison with the measurements done on the inoculated set of copolymers.

4 Results

4.1 Hydrogel swelling equilibrium

Figure 2 shows the swelling equilibrium measurements obtained from the HEMA and PEGDMA hydrogels when they were copolymerized with varying proportions of SEMA or MEATAC monomers. At low ion strengths, hydrogels fabricated with HEMA and either SEMA or MAETAC showed charge-dependent swelling. Hydrogels fabricated with PEGDMA and either SEMA or MAETAC, however, exhibited little or no swelling as a function of the added charged monomers. Figure 2 shows a correction for swelling on the actual charge density, assuming 100% incorporation of the charged monomer during the hydrogel synthesis. As a result of the swelling,

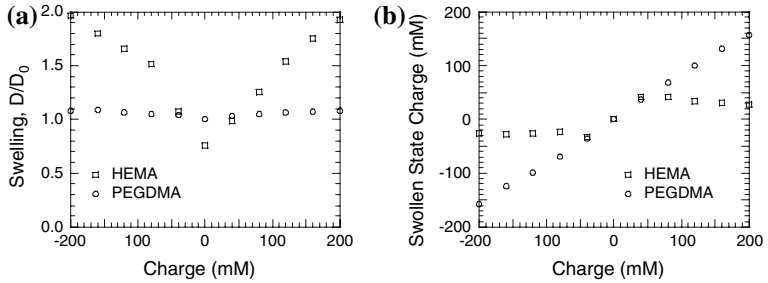

Fig. 2 Hydrogel swelling and charge density at low ionic strengths. (**a**) Experimental measurements of HEMA and PEGDMA copolymer swelling show very different patterns. The HEMA copolymer polyelectrolyte hydrogels are consistent with increasing osmotic pressures produced by charged monomeric groups. The PEGDMA hydrogels are relatively unresponsive. (**b**) Assuming that all monomeric groups are polymerized into the network, the actual charge, corrected for swelling, indicates that the PEGDMA hydrogels are more charged than the swollen HEMA copolymer hydrogels

the HEMA polyelectrolyte hydrogel charges were significantly smaller than the prepared charge.

Figure 3 shows the swelling equilibrium phase transitions of HEMA and PEGDMA copolymer polyelectrolyte hydrogels as a function of bath NaCl concentration. Hydrogels fabricated with HEMA displayed typical polyelectrolyte behavior and exhibited deswelling transitions with increasing bath NaCl concentration. The PEGDMA hydrogels, however, show little change in swelling over the range of bath NaCl concentrations.

Figure 4 summarizes the swelling equilibria at physiologic ion strengths. Compared to Fig. 1, where the swelling and effective charge estimates were made in distilled deionized water, the swelling was less, but the effective charge was greater as a result of the deswelling produced by the bath ions. Notice that, assuming efficient copolymerization, the effective charge on the PEGDMA copolymer hydrogels increases much more rapidly than that of the corresponding copolymer HEMA hydrogels because of the restricted swelling. To confirm the presence of charge in this case, additional measurements, such as membrane potential measurements, should be included.

Figure 5 summarizes a sequence of theoretical predictions that illustrate the effect of charge on swelling behavior. For a free swelling hydrogel, increasing charge produces increasing swelling states at low ionic strengths. Increasing the bath salt concentration, however, leads to deswelling transitions as a result of, a decreasing net osmotic pressure. The swelling states in this model are dependent only on the magnitude and not on the sign, of the charged monomer concentration. These predictions are in qualitative agreement with the HEMA copolymer swelling transitions.

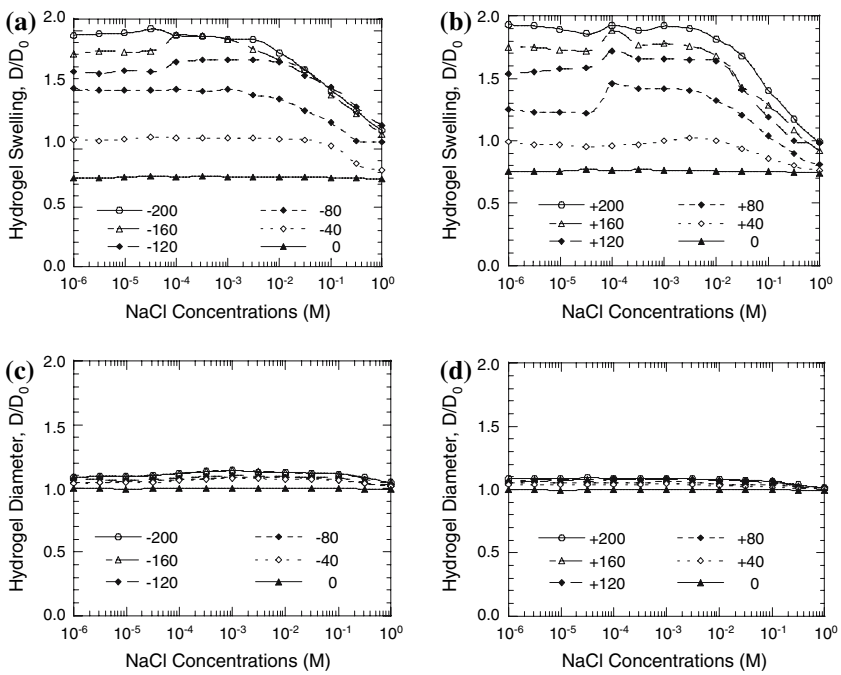

Fig. 3 The equilibrium swelling transitions of HEMA and PEGDMA polyelectrolyte copolymers as a function of bath NaCl concentration and prepared monomer charge density. (**a**) The HEMA–SEMA and (**b**) HEMA–MAETC copolymer hydrogels exhibit typical polyelectrolyte hydrogel behavior and have deswelling transitions with increasing bath salt concentration. The PEGDMA–SEMA (**c**) and PEGDMA–MAETAC (**d**) hydrogels, however, are relatively unresponsive to changes in the bath NaCl concentration

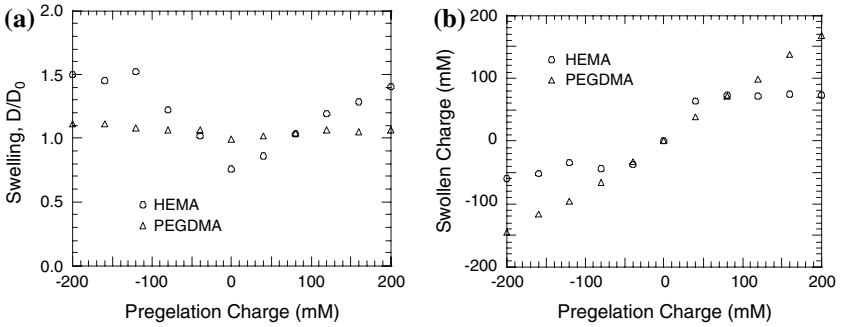

Fig. 4 Swelling equilibria and effective charge at physiologic ion strengths for HEMA and PEGDMA copolymer polyelectrolyte hydrogels as a function of initially prepared charge. (**a**) The swelling equilibria are diminished compared to that obtained in distilled deionized water as a result of ionic screening. (**b**) The charge, corrected for swelling and assuming 100% polymerization efficiency, is less at physiologic ion strengths for the swollen HEMA hydrogels compared to the PEGDMA hydrogels

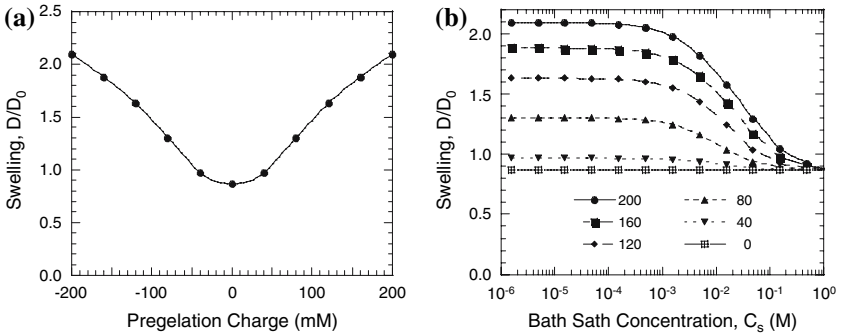

Fig. 5 Theoretical swelling predictions as a function of charge offset and bath salt concentration. (**a**) At low bath ionic strengths, the hydrogel swells with increasing negative or positive charge. (**b**) Increasing the bath salt concentration produces deswelling transitions for hydrogels with charged monomers. Greater deswelling transitions are observed for hydrogels with greater charged monomer concentrations. Other factors, such as entanglement and polydispersity, can complicate the swelling behavior

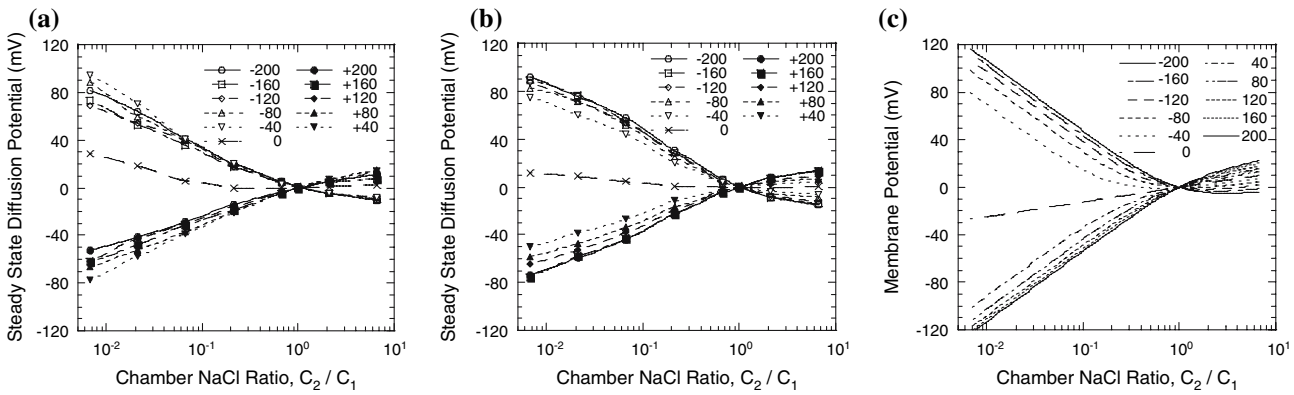

Fig. 6 Hydrogel steady-state membrane potentials for (**a**) HEMA and (**b**) PEGDMA copolymer polyelectrolyte hydrogels. The membrane potential curves for both these polyelelectrolyte hydrogels are consistent with the incorporation of charge into the hydrogel network. (**c**) Theoretical predictions are in qualitative agreement

4.2 Non-equilibrium steady-state membrane potentials

Figure 6 shows the steady state membrane potentials of the HEMA and PEDGMA copolymer polyelectrolyte hydrogels. Both sets of hydrogels show patterns consistent with incorporated charge. The HEMA copolymer membrane potentials, however, display a more complicated pattern of membrane potentials as a result of charge density changes associated with swelling. It is important to appreciate that concentration-dependent swelling can produce a spatially

dependent charge density through the membrane. Although the PEGDMA copolymer polyelectrolyte hydrogels did not exhibit swelling transitions with added charged monomers, the membrane potential measurements were consistent with the presence of network charge. Stagnant boundary layers and other artifacts appeared to distort the membrane potential measurements at low ionic strengths. No significant changes were observed by the presence or absence of attached cells or serum containing media.

4.3 Cellular proliferation and morphology

Figure 7 shows the proliferation of endothelial cells on copolymer HEMA or PEGDMA polyelectrolyte hydrogels as a function of the initially prepared charge. The actual charge, corrected for swelling at physiologic ion strengths, can be seen in Fig. 4b. The error bars shown in each plot represent the variability among a total of nine different images where three images were taken from three different hydrogels.

Rapid growth patterns were observed for HEMA copolymer hydrogels with charge concentrations of –120, –160, and –200 mM while cells eventually died and sloughed off hydrogels with the charge concentrations of 0, –40, and –80 mM. Copolymers with a –120 mM charge displayed a great deal of variability among the three hydrogel sample sets. Positively charged HEMA hydrogels appear to exhibit a critical concentration of charged monomers that lead to confluent endothelial monomers. Hydrogels with initially prepared positive charge concentrations greater than or equal to 120 mM produced relatively rapid attachment and proliferation patterns.

The PEGDMA based hydrogels were more resistant to endothelial cell growth and proliferation. The copolymers with higher charge concentrations supported initial endothelial cell attachment, but those cells eventually rounded up and formed cell aggregates. The standard deviation of the cell covered area estimates among representative pictures for these hydrogels was also relatively large.

Figures 8 and 9 illustrate a representative set of endothelial cell morphology patterns on negatively charged, neutral, and positively charged hydrogel copolymers of HEMA and PEGDMA. Negatively charged HEMA hydrogels promoted cellular attachment and spreading of spindle-like cellular structures. The neutral HEMA hydrogel was relatively resistant to cellular attachment. The positively charged HEMA hydrogel promoted the growth of cobblestone-like patterns of endothelial cell attachment. The negative, neutral and positively charged PEGDMA hydrogels remained resistant to cellular attachment.

5 Discussion

The use of synthetic hydrogels to mimic the endothelial cell basement membrane has many important applications in biotechnology and medicine. Synthetic hydrogel matrices with differing compositions can simulate the underlying substratum found in vivo and provide an in vitro model for cellular growth and proliferation as a

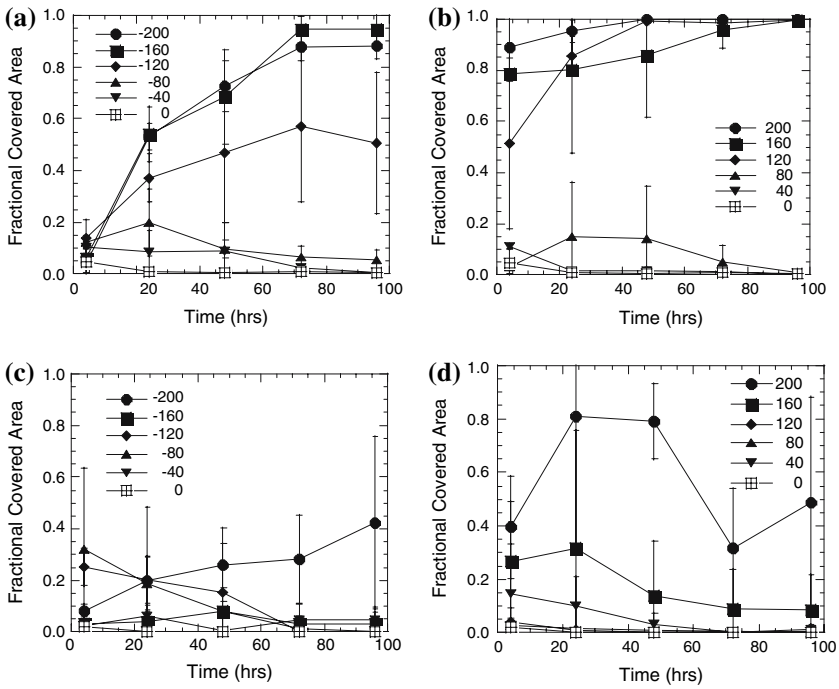

Fig. 7 Endothelial proliferation on HEMA and PEGDMA polyelectrolyte hydrogels. (**a**) Copolymer HEMA–SEMA polyelectrolyte hydrogels show an increase in attachment when the initially prepared hydrogel charge density reaches –120 mM. (**b**) Copolymer HEMA–MAETAC hydrogels exhibit a well-defined increase in proliferation rates when the initially prepared charge density reaches +120 mM. (**c**) Copolymer PEGDMA–SEMA hydrogels show a weak pattern of endothelial cell attachment and proliferation. (**d**) Copolymer PEGDMA–MAETAC hydrogels only allow attachment for prepared charge densities reaching +200 mM

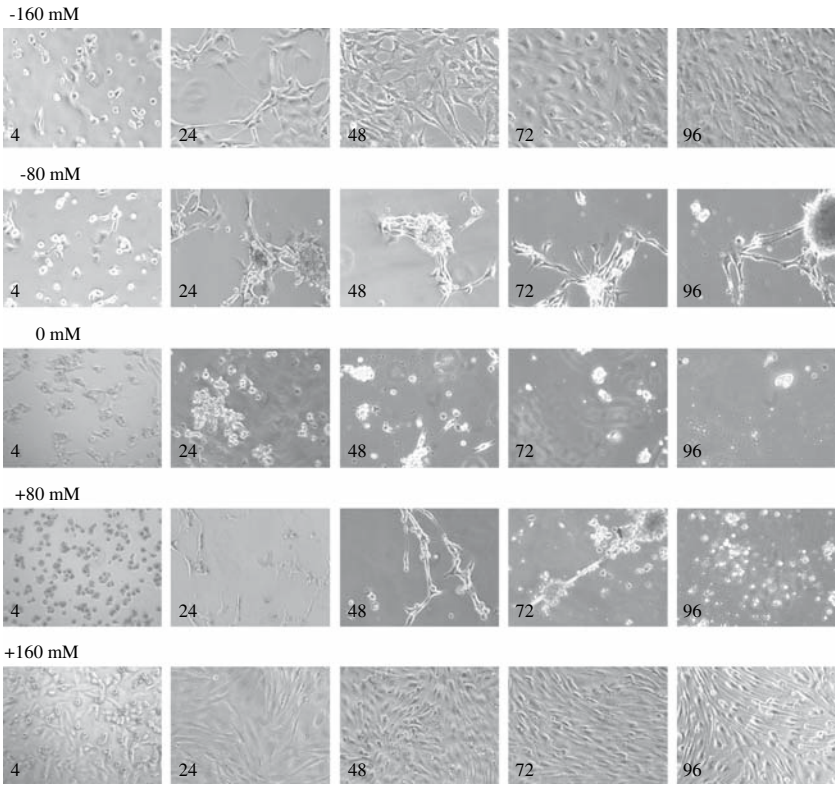

Fig. 8 Representative endothelial cell morphologies on negative, neutral, and positively charged HEMA copolymer hydrogels at 4, 24, 48, 72, and 96 h of growth. Neutral and weakly charged HEMA hydrogels do not promote cellular attachment. A sufficient amount of either negative or positive charge, however, promotes cellular attachment and proliferation

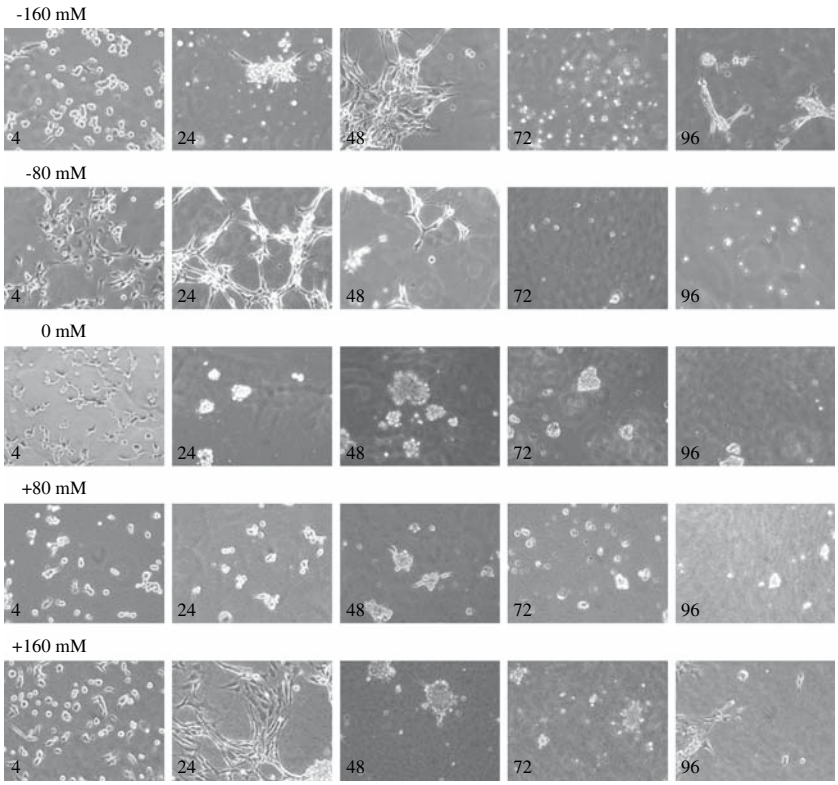

Fig. 9 Representative endothelial cell morphologies on negative, neutral, and positively charged PEGDMA copolymer hydrogels at 4, 24, 48, 72, and 96 h of growth. These hydrogels resist cellular attachment and growth compared to the HEMA hydrogels. Large charge offsets promote an initial attachment. In most cases, however, the cells eventually detach and die

function of matrix composition. Adding charged monomeric groups is often used to promote cellular adhesion and proliferation. In general, however, increasing the relative proportion of charged monomers can produce a complex pattern of phase transitions that can alter the expected charge density. The two copolymers considered in this

study, for example, illustrate two very different patterns of phase behavior and cellular responses.

Understanding the effects of charge on cellular adhesion, morphology, and proliferation begins with a careful consideration of the phase changes produced by adding charged monomers to the hydrogel network. As this study shows, the hydrogel network charge density at physiologic ion strengths depends on the degree of swelling, dissociation equilibrium, synthesis conditions and a number of other factors. Charge density estimates of free swelling hydrogels, such as the HEMA copolymers considered in this study, can be obtained by correcting the initial charge monomer concentration for swelling transitions. Non-equilibrium membrane potential methods provide an alternative method for hydrogels, such as the PEGDMA copolymers, that do not undergo free swelling transitions. These equilibrium and non-equilibrium methods, therefore, complement each other.

The use of the Nernst–Plank equations to develop a theoretical model, commonly known as the Teorell [15] Meyer-Sievers [16] (TMS) model, is prevalent in the literature [17–20]. This theory couples diffusion and Donnan potentials to account for ion transport across homogeneously charged membranes. By assuming that the perturbing electric field is much smaller than the double layers established at the hydrogel and solution boundary, boundary conditions can be determined using an equilibrium ion exchange approach. Before a comparison of the theoretical curves with the experimental data is made, it is important first to obtain swelling curves for the membranes to determine what effect the salt concentration gradients have on the swelling behavior and how this will affect the internal net charge inferred from the membrane potential measurements. Thus, it is beneficial to use some form of swelling measurements and theory as a comparison with the charge predictions obtained from the TMS model. Each of these models can then be evaluated and the results compared to assess the net membrane charge.

The combination of swelling and membrane potential measurements is consistent with the successful incorporation of charged groups into both the HEMA and PEGDMA copolymer hydrogel structures. Although the PEGDMA hydrogels did not show swelling and deswelling transitions characteristic of charged polyelectrolytes, the membrane potential measurements were consistent with the presence of fixed charge groups. The PEGDMA network appeared to have maintained the charge density at preparation by preventing swelling transitions produced by repulsive osmotic pressures. Both swelling and membrane potential were, therefore, necessary in this study to confirm and quantify the actual charge present. Swelling and the difference in the monomer chemical reactivities can alter the actual charge density from that used in the hydrogel preparation.

Figures 1 and 2 provide an experimentally supported justification for ignoring the effects of ion dissociation. At low ionic strengths, acid or base dissociation will produce deswelling transitions [6–8]. The absence of acid and base dissociation effects in this study are consistent with the large acidic and base dissociation constants associated with the sulfonic acid and quaternary ammonium chloride functional groups. Ignoring ion dissociation equilibrium, however, cannot always be justified. Carboxyl and tertiary ammonium chlorides, for example, may not be completely dissociated. In addition, at high charge densities, ion condensation effects can limit the total charge density [21].

The incorporation of charge into cellular scaffolds can influence cellular adhesion and growth as a result of non-specific interactions and/or by altering the types and amounts of serum proteins adsorbed on the copolymers that serve as cellular adhesive contacts. Non-specific and specific interactions that lead to cell spreading on a material have been directly correlated with proliferation rates [22, 23]. In particular, the influence of positively and negatively charged functional groups on cellular adhesion and proliferation has been the subject of intense research. Although results vary from study to study, the incorporation of positive or negative functional groups into hydrogel matrices encourages cellular attachment and growth.

By incorporating different molar concentrations of SEMA and MAETAC to offset the HEMA or PEGDMA neutral background, linearly charged copolymer hydrogels from 0 to ±200 mM, in increments of 40 mM, were initially prepared. The SEMA acidic monomer, the MAETAC basic monomer, and the HEMA neutral monomer integrated the functional groups $–SO_3H$, $(CH_3)_3N–$, and –OH, respectively, into the matrix. Upon equilibration in physiologic solutions, however, swelling transitions in the HEMA copolymers reduced the effective charge compared to the charge density in the unswollen PEGDMA copolymer series. As Fig. 4 shows, preparing copolymer hydrogels with charge densities greater than 80 mM produced swelling transitions that kept the effective charge density around 70 mM for the HEMA series. Because the PEGDMA hydrogel series did not appreciably swell with increasing charged monomer concentration, however, a proportional increase in the effective charge resulted, with increasing prepared charged monomer concentration. Although the HEMA copolymer series had a reduced effective charge because of swelling transitions, this series promoted the attachment of cells to a greater extent than did the analogous PEGDMA hydrogel series, which maintained the prepared charge as a result of restricted swelling.

Copolymer hydrogels made of 2-hydroxy ethylmethacrylate (HEMA) and incorporated functional groups such as –COOH, $–SO_3H$, and $(CH_3)_nN$-support various amounts of

cellular growth depending on the charge density integrated into the matrix, the amount of protein adsorbed to the copolymer surface, and the hydrophilic properties of the matrix [1, 24, 25]. The presence of ionizable functional groups in HEMA hydrogels appears to be essential for cell adhesion and spreading [24]. Copolymers containing moderate to high concentrations of poly(ethylene glycol) dimethacrylate (PEGDMA) discourage protein adsorption and cellular attachment and growth [26–29]. Increasing amounts of incorporated PEGDMA caused decreasing cellular adhesion and decreased protein adsorption [1, 30, 31].

6 Conclusion

A combination of both swelling and membrane potential measurements and analysis is necessary to be able to quantify the effects of hydrogel charge density on cellular attachment and proliferation. In this study, cellular attachment and proliferation increased with increasing proportions of charged monomers and showed a threshold pattern of attachment and growth on the positive charged HEMA–MAETAC copolymer hydrogels with increasing proportions of initially prepared charge. The series of PEGDMA copolymer hydrogels remained relatively resistant to cellular attachment and proliferation over the range of prepared charges.

Acknowledgements This work was supported in part by a National Science Foundation CAREER Award BES-0238905 (AE) and in part by an American Heart Association Award 0265029B (AE).

References

1. P. B. VAN WACHEM, A. H. HOGT, T. BEUGELING, J. FEIJEN, A. BANTJES, J. P. DETMERS and W. G. VAN AKEN, *Biomaterials* **8** (1987) 323
2. Y. M. CHEN, N. SHIRAISHI, H. SATOKAWA, A. KAKUGO, T. NARITA, J. P. GONG and Y. OSADA, *Biomaterials* **26** (2005) 4588
3. C. BOURA, S. MULLER, D. VAUTIER, D. DUMAS, P. SCHAAF, J. C. VOEGEL, J. F. STOLTZ and P. MENU, *Biomaterials* **26** (2005) 4568
4. A. E. ENGLISH, E. R. EDELMAN and T. TANAKA, in "*Experimental Methods in Polymer Science*", edited by T. Tanaka (Academic Press, Cambridge, 2000), p. 547
5. A. E. ENGLISH, S. MAFE, J. A. MANZANARES, X. YU, A. Y. GROSBERG and T. TANAKA, *J. Chem. Phys.* **104** (1996) 8713
6. A. E. ENGLISH, T. TANAKA and E. EDELMAN, *J. Chem. Phys.* **105** (1996) 10606
7. A. E. ENGLISH, T. TANAKA and E. EDELMAN, *Macromolecules* (1998) 1989
8. A. E. ENGLISH, T. TANAKA and E. R. EDELMAN, *J. Chem. Phys.* **107** (1997) 1645
9. A. E. ENGLISH, T. TANAKA and E. R. EDELMAN, *Polymer* (1998) 5893
10. G. I. BELL, M. DEMBO and P. BONGRAND, *Biophys. J.* **45** (1984) 1051
11. D. A. HAMMER and D. A. LAUFFENBURGER, *Biophys. J.* **52** (1987) 475
12. M. DEMBO, D. C. TORNEY, K. SAXMAN and D. HAMMER, *Proc. Roy. Soc. Lond. B* **234** (1988) 55
13. M. D. WARD and D. A. HAMMER, *Biophys. J.* **64** (1993) 936
14. H. B. CALLEN, *Thermodynamics* (John Wiley & Sons, Inc., New York, 1960), p. 376
15. T. TEORELL, *Proc. Soc. Exp. Biol. Med.* **33** (1935) 282
16. K. H. MEYER and J.-F. SIEVERS, *Helv. Chim. Acta* **19** (1936) 649
17. R. TELARANTA, J. A. MANZANARES and K. KONTTURI, *J. Electroanal. Chem.* **464** (1999) 222
18. M. HIGA, A. TANIOKA and A. KIRA, *J. Memb. Sci.* **140** (1998) 213
19. S. KOTER, *J. Memb. Sci.* **108** (1995) 177
20. Y. TOYOSHIMA and H. NOZAKI, *Phys. Chem.* **74** (1970) 2704
21. F. OOSAWA, *Polyelectrolytes* (M. Dekker, New York, 1971)
22. J. FOLKMAN and A. MOSCONA, *Nature* **273** (1978) 345
23. A. BEN-ZE'EV, *J. Cell Biol.* **97** (1983) 858
24. P. R. BERGETHON, V. TRINKAUS-RANDALL and C. FRANZBLAU, *J. Cell Sci.* **92** (1989) 111
25. K. SMETANA Jr., J. VACIK, D. SOUCKOVA, Z. KRCOVA and J. SULC, *J. Biomed. Mater. Res.* **24** (1990) 463
26. P. D. DRUMHELLER and J. A. HUBBELL, *Anal. Biochem.* **222** (1994) 380
27. D. W. BRANCH, B. C. WHEELER, G. J. BREWER and D. E. LECKBAND, *Biomaterials* **22** (2001) 1035
28. E. TZIAMPAZIS, J. KOHN and P. V. MOGHE, *Biomaterials* **21** (2000) 511
29. M. ZHANG, T. DESAI and M. FERRARI, *Biomaterials* **19** (1998) 953
30. B. S. JACOBSON, *Tissue Cell* **14** (1982) 69
31. K. IIO, N. MINOURA, S. AIBA, M. NAGURA and M. KODAMA, *J. Biomed. Mater. Res.* **28** (1994) 459